ℓ_1-Sparse Reconstruction of Sharp Point Set Surfaces

HAIM AVRON
Tel-Aviv University and IBM T.J. Watson Research Center
ANDREI SHARF
Ben-Gurion University
CHEN GREIF
University of British Columbia
and
DANIEL COHEN-OR
Tel-Aviv University

We introduce an ℓ_1-sparse method for the reconstruction of a piecewise smooth point set surface. The technique is motivated by recent advancements in sparse signal reconstruction. The assumption underlying our work is that common objects, even geometrically complex ones, can typically be characterized by a rather small number of features. This, in turn, naturally lends itself to incorporating the powerful notion of sparsity into the model. The sparse reconstruction principle gives rise to a reconstructed point set surface that consists mainly of smooth modes, with the residual of the objective function strongly concentrated near sharp features. Our technique is capable of recovering orientation and positions of highly noisy point sets. The global nature of the optimization yields a sparse solution and avoids local minima. Using an interior-point log-barrier solver with a customized preconditioning scheme, the solver for the corresponding convex optimization problem is competitive and the results are of high quality.

1. INTRODUCTION

Scanning devices have turned in the course of the last few years into commercial off-the-shelf tools. Current scanners are capable of producing large amounts of raw, dense point sets. One of today's principal challenges is the development of robust point processing and reconstruction techniques that deal with the inherent noise of the acquired dataset.

Early point set surface methods [Alexa et al. 2003; Pauly et al. 2003; Amenta 2004; Kolluri 2005] assume the underlying surface is smooth everywhere. Hence, robustly reconstructing sharp features in presence of noise is more challenging. To account for sharp features and discontinuities, advanced methods rely on explicit representations of these characteristics [Adamson and Alexa 2006; Guennebaud and Gross 2007], use anisotropic smoothing [Fleishman et al. 2003; Jones et al. 2003], robust statistics [Fleishman et al. 2005; Oztireli et al. 2009] or feature-aware methods [Lipman et al. 2007a]. These methods are typically fast, but they employ their operators locally and do not seek an objective function with a global optimum.

In this work, we introduce a technique based on a global approach that utilizes sparsity. Our method is motivated by the emerging theories of sparse signal reconstruction and compressive sampling [Donoho et al. 2006; Candes et al. 2006]. A key idea here is that in many situations signals can be reconstructed from far fewer data measurements compared to the requirements imposed by the Nyquist sampling theory. In sparse signal reconstruction, instead of using an overcomplete representation, the reconstruction contains

the sparsest possible representation of the object. This technique can become effective in the context of surface reconstruction, since common objects can often be characterized in terms of a rather small number of features, even if they are geometrically complex.

Our method is inspired by ℓ_1 minimization in sparse signal reconstruction and feature selection. We use the ℓ_1-sparsity paradigm since it avoids one of the main pitfalls of methodologies such as least squares, namely smoothed out error. Indeed, the ℓ_2 norm tends to severely penalize outliers and propagate the residual in the objective function uniformly. Hence, the solution is typically of a very poor degree of sparsity. Since least squares methods by their nature handle smooth surfaces better than nonsmooth ones, common techniques that use them must rely on working in a locally smooth fashion.

The last observation is particularly important for objects with sharp features. An ℓ_1-based method such as the one we introduce is not restricted by the aforementioned locality limitations that ℓ_2 entails. Since outliers are not excessively penalized, most of the "energy" of the residual in the objective function is expected to be concentrated near the sharp features. Thus, by minimizing the objective function in the ℓ_1 sense we encourage sparsity of nonsmooth singularities in the solution. The ℓ_1 norm is not differentiable, and formulations associated with it are harder to solve, compared to ℓ_2-based formulations. Nevertheless, the objective function is convex and as long as convexity is preserved, it is well understood how to solve the problem in hand, and efficient solvers are available. Theory and applications based on ℓ_1-sparsity have been enjoying a huge boost in the last few years in the scientific community at large. Motivated by this success we seek to utilize ℓ_1-sparsity in computer graphics. In this work we use ℓ_1-sparsity to build a novel method for reconstructing point set surfaces with sharp features.

Our global reconstruction method incorporates also inequality constraints that ensure that the points are sufficiently close to the original input. We first solve for the point orientations, and then, based on the piecewise smooth normals, solve for the point positions. We show that we reconstruct point sets effectively, and compare our technique to state-of-the-art methods by running on synthetic models as well as real scanned models.

This work offers two main contributions. First is the formulation of a global ℓ_1-sparse optimization problem for 3D surfaces. We show that sparsity and ℓ_1-minimization are highly effective in surface reconstruction of real scanned objects. Second, we show that this problem can be solved efficiently by convex optimization techniques. We demonstrate that our method runs on large datasets within a reasonable time.

2. RELATED WORK

In this section we provide a review of relevant work separated into two parts. First, we focus on surface reconstruction methods in the context of sharp feature approximation. Then, we review methods for sparse signal reconstruction and total variation.

2.1 3D Surface Reconstruction

Since the early 1990s, there has been a substantial amount of work in the domain of surface reconstruction from range scanned data.

Moving Least Squares (MLS) [Shepard 1968] is a classical and popular method for functional approximation. Levin [2003] and Alexa et al. [2003] have demonstrated its effectiveness and promise for representing point set surfaces. A number of papers have followed, improving and extending the MLS operator; see Alexa and

Adamson [2004], Amenta [2004], Amenta and Kil [2004], Shen et al. [2004], Dey and Sun [2005], and Kolluri [2005]. At the core of these methods is an iterative projection that involves a local optimization to find the (local) reference plane and a bivariate polynomial fitting. Although state-of-the-art MLS-based methods handle nonuniform data and noise, these methods are limited by the locality of the operator.

MLS-based techniques are ideally designed to reconstruct smooth surfaces. To reconstruct sharp features, various approaches have been proposed. Methods that rely on an explicit representation of sharp features [Reuter et al. 2005; Adamson and Alexa 2006, Guennebaud and Gross 2007] classify the input samples into piecewise linear components to model sharp features. A more challenging task is to automatically detect and reconstruct features present in noisy point clouds in a global framework.

Several feature-aware filters have been developed for 3D mesh denoising and smoothing [Fleishman et al. 2003; Jones et al. 2003]. Following image denoising approaches [Tomasi and Manduchi 1998], they use an underlying Gaussian smoothing kernel that accounts for position and normal similarity in a continuous manner. Samples across a sharp feature can be seen as outliers, and robust statistics-based methods are presented in Mederos et al. [2003] to locally deal with those outliers and reconstruct sharp features. Similarly, Fleishman et al. [2005] derive an iterative refitting algorithm that locally classifies the samples across discontinuities by applying a robust statistics framework. More recently, Daniels et al. [2007], Oztireli et al. [2009], Lipman et al. [2007a, 2007b] have presented robust methods for surface reconstruction from point clouds, which handle sharp features and noise. Common to all these methods is their locality approach; both detection and reconstruction of sharp features are performed within a local context. This leads to the possible detection of local minima, where locally, high noise-to-signal ratio yields redundant features or in the other extreme oversmoothing. This phenomena is demonstrated in Figure 4 (middle row), which shows the result of applying a bilateral filter (local method) on a shallow V-shaped noisy model. In contrast, we apply a global method that solves for the whole surface at once, avoiding such effects and generating a global optimal solution that preserves the sharp features (bottom row).

Note that some of the local methods discussed before use some form of ℓ_1-norm minimization. Nevertheless, this usage is fundamentally different from our method. In these methods ℓ_1 minimization is applied as a robust statistic, based on the observation that data across discontinuity can be viewed as outliers. Thus, the ℓ_1 minimization is used to make the local filter more robust. Nevertheless, their local nature poses inherent limitations. In contrast, our method is based on the ℓ_1-sparsity paradigm (discussed in Section 3) which naturally leads to a global method.

Somewhat similar to us, Sharf et al. [2008] have recently used a lower-than-ℓ_1 minimization scheme which they apply to dynamic surface reconstruction. The problem is formulated as an implicit incompressible flow volume minimization which accounts for volume boundaries using a reweighted $\ell_{0.8}$ norm. Both works have in common the observation that a metric below ℓ_2 better accounts for sharp features.

2.2 Sparse Signal Reconstruction

Sparse signal processing has had over the last few years a significant impact on many fields in applied science and engineering such as statistics, information theory, computer vision, and others. From a general viewpoint, sparsity and compressibility lead to dimensionality reduction and efficient modeling.

The general idea of ℓ_1 regularization for the purpose of sparse signal reconstruction or feature selection has been used in geophysics since the early 1970s; see, for example, Claerbout and Muir [1973]. In signal processing, the idea of ℓ_1 regularization comes up in several contexts, including basis pursuit [Chen et al. 2001] and image decomposition [Elad et al. 2005; Starck et al. 2005]. In these works it is shown that while the ℓ_2 norm yields a minimum length solution, it lacks properties of sparsity and the reconstructed signal error is spatially spread out. Although ℓ_0 is in fact the sparsest solution, in Donoho et al. [2006] it is shown that under bounded noise conditions, the recovered sparse representation using ℓ_1 is both correct and stable. Similar to us, Tropp [2006] shows that convex optimization techniques are useful for sparse signal reconstruction.

The ℓ_1-sparsity paradigm has been applied successfully to image denoising and deblurring using Total Variation (TV) methods [Rudin 1987; Rudin et al. 1992; Chan et al. 2001; Levin et al. 2007]. The underlying model for TV methods aims at exploiting the sparsity of the gradient of the image. The continuous variant yields a model of a nonlinear PDE, hence is less relevant in the context of the current work. The discrete variant, on the other hand, yields the convex objective function

$$TV(u) = \Sigma_{ij} \| D_{ij} u \|_2,$$

where D_{ij} is the discrete gradient operator at pixel (i, j) and u is a vector containing the gray-level pixel values. TV methods filter the image by minimizing $TV(u)$ under a certain constraint, for example, one that keeps the output sufficiently close to the input.

$$\| u - u_0 \|_2 \leq \varepsilon$$

TV is designed for images, and hence is not directly applicable to our problem. Our method is close in spirit to TV. Similar to their sparse gradient minimization, we formulate our piecewise smoothness reconstruction problem as a sparse minimization of orientation differences and position projections.

The analog of TV for surface denoising is Total Curvature (TC), which corresponds to minimizing the integral of the local curvature values [Tasdizen et al. 2002, 2003; Elsey and Esedoglu 2009]. TC methods preserve edges and sharp features, but by their nature, being represented by a nonlinear PDE, they require significant computational resources and an underlying parametrization. Given the nature of TC, it seems hard to develop a convex discrete variant for it.

Rather than working on curvatures, we examine the normal field of the surface. This allows us to develop a convex ℓ_1-based formulation. It should be stressed that convexity is of much importance, since it gives rise to a robust, efficient, and stable solution procedure in contrast to nonconvex nonlinear problems such as the just mentioned.

3. ℓ_1-SPARSITY OVERVIEW

Suppose we are given discrete samples of a continuous time signal $u(t)$. Signal reconstruction deals with the problem of reconstructing u from those samples as a linear combination of basis functions $\phi_i \in \mathbb{R}^n$, $i = 1, \ldots, m$, with $m > n$. The problem amounts to finding the coefficients α_i such that

$$u = \sum_{i=1}^{m} \alpha_i \phi_i.$$

The Nyquist sampling theorem states that the number of samples needed to reconstruct a signal without error is dictated by its bandwidth. Inside the bandwidth the signal can be dense, containing information in all frequencies. Nevertheless, it has been shown in a set of seminal papers [Candes et al. 2006; Donoho et al. 2006] that when the signal is sparse, that is, only a small set of frequencies are present, the signal can be reconstructed from a number of samples much lower than required by Nyquist's theorem using ℓ_1 minimization.

Sparse signal reconstruction utilizes the fact that if the underlying signal indeed has a sparse representation, then its coefficients α can be cast as the solution of the optimization problem. We have

$$\min_{\alpha} \|\alpha\|_0 \quad \text{s.t.} \quad u(t_j) = \sum_{i=1}^{m} \alpha_i \phi_i(t_j),$$

where the samples are given at times t_j. The zero norm, $\|.\|_0$, represents the number of nonzero elements in a vector. Unfortunately, formulating the problem in terms of this norm requires a combinatorial solution time; the problem is highly nonconvex. It is thus common practice to replace ℓ_0 by (the convex) ℓ_1 norm. It has been shown [Candes et al. 2006; Donoho et al. 2006; Tropp 2006] that in some cases minimizing the ℓ_1 norm is equivalent to minimizing the ℓ_0 norm.

It is well established in the scientific community that in presence of discontinuities, ℓ_2 minimization tends to produce solutions that are smooth. To overcome this problem, the iterative reweighted ℓ_2 minimization (IRLS) method has been introduced [Holland and Welsch 1977] that achieves lower-than-ℓ_2-sparsity using a predesigned reweighting scheme. The weights essentially concentrate the error at discontinuities and enhance sparsity. Formulating an ℓ_1 minimization scheme instead achieves sparsity in a much more direct way. Although theoretically ℓ_1 minimization can be approximated using IRLS, interior-point methods (like the one we use) are usually faster and more reliable in terms of convergence and stability.

Sparse reconstruction is a broad methodology with many flavors. In some application areas, the basis functions are either known or predefined by the method. In these cases it is often possible to establish formal guarantees on the reconstruction. The most notable is compressive sampling which economically translates data into a compressed digital form subject to ℓ_1 minimization; for a survey see Candes and Wakin [2008]. Other sparse reconstruction methods, and most notably TV filters, do not assume a predefined overcomplete dictionary. Instead, these methods assume sparsity under some transformation, and set up an optimization scheme that filters the signal using the sparsity prior.

Our method is inspired by sparse ℓ_1 filtering methods like TV. As already mentioned, given that our scan data is sampled from a piecewise smooth shape, we seek to approximate it by a sparse set of smooth pieces that connect at the edges. We approximate smoothness in terms of pairwise orientation differences; next, positions are integrated from orientations by assuming local planarity. We provide the exact details of our formulation in the next section.

It is important to discuss the relationship between ℓ_1 minimization and sparse methods. Broadly speaking, there are two major research domains where ℓ_1 minimization has been extensively applied: robust statistics (i.e., as an M-estimator) and sparse recovery. Robust statistics use ℓ_1 due to its robustness to outliers. Sparse recovery methods use ℓ_1 as an approximation of ℓ_0. The problem is formulated such that the solution is a sparse vector, and ℓ_1 is used to find a sparse-as-possible approximation. Our method belongs to the latter class of methods.
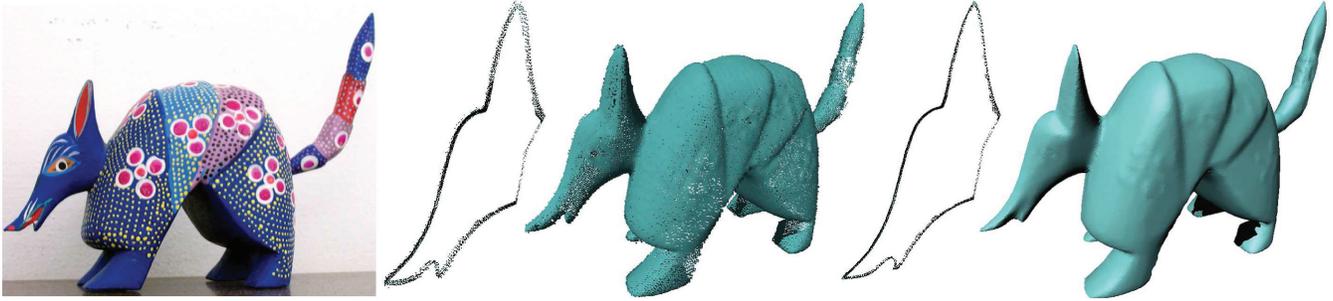
Fig. 1. A demonstration of the effectiveness of our ℓ_1-sparsity-based approach on a scanned model. The armadillo statue (left) is scanned generating a noisy point cloud (middle). Using our method we are able to reconstruct it and recover its sharp features (right). Close-up view of a cross section of its head reveals the sharpness of the reconstructed surface.
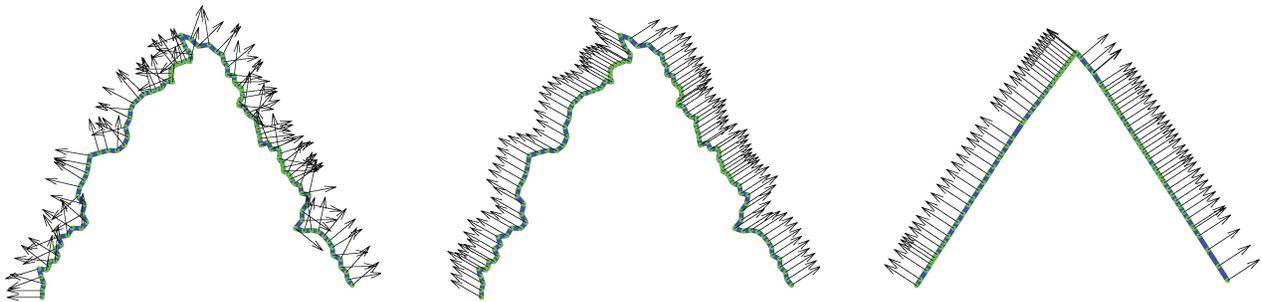

Fig. 2. A 2D demonstration of our ℓ_1-sparse reconstruction method applied to a synthetic V-shaped model. Given a 2D noisy curve (left), the point orientations are solved first, using an interior-point solver (middle). In the second step, the correctly computed orientations are used to recover consistent positions. The rightmost figure is the V-shape result of our algorithm.

4. RECONSTRUCTION MODEL

Since scanned information is generally noisy, we cannot assume that we have high-quality point orientations, and rely on that in our solution procedure. Hence, similarly to Lipman et al. [2005], we decouple orientations and positions. We solve first for the orientations, and then use them to compute consistent positions. We formulate both problems in a similar ℓ_1 nature, yielding a consistent solution. For a 2D demonstration of this process see Figure 2.

Our goal is to formulate a global surface approximation that is piecewise smooth and consists of a sparse set of singularities at sharp edges. We denote as $P(X, N)$ a point cloud defined by positions $x_i \in X \subseteq \mathbb{R}^3$ and corresponding orientations $n_i \in N \subseteq \mathbb{R}^3$. Thus, a point is defined by the pair $p_i = (x_i, n_i)$.

Our orientation reconstruction model is based on the same key observation made by Tasdizen et al. [2003]: smooth surfaces have smoothly varying normals, thus penalty functions should be defined on the surface normals. However, their method assumes a local parametrization of the surface and involves solving second-order PDEs. These limitations have led us to adopt a simplified generic approach. Instead of using a quadratic form for curvature, we use pairwise normal differences as an estimator for shape smoothness. If two points p_i and p_j belong to the same smooth part, and the distance between them is small enough in local feature size, then $n_i \approx n_j$. Furthermore, we assume that there is a minimum crease angle at singularities between smooth parts. Hence, at crease angles where p_i and p_j belong to different smooth parts, the distance between n_i and n_j is above a small threshold τ. This leads to

an observation that the reconstructed normals should be such that only a small (i.e., sparse) number of local normal differences are large.

We use computed orientations to define consistent positions by assuming that the surface can be approximated well by local planes. Given a pair of neighbor points (p_i, p_j), we examine $n_{ij} \cdot (x_i - x_j)$ (where n_{ij} is the average normal). Indeed, if both p_i and p_j belong to a smooth part of the surface then $n_{ij} \cdot (x_i - x_j) \approx 0$. At sharp features we expect $\left| n_{ij} \cdot (x_i - x_j) \right| > 0$.

Note that this last assumption is not necessarily true and in some point configurations $n_{ij} \cdot (x_i - x_j) \approx 0$ even at sharp features (e.g., p_i and p_j are equidistant from both sides of a sharp perpendicular edge). Nevertheless, such specific configurations do not occur much in practice and the use of large neighborhoods for each point compensates for this discrepancy.

In the following subsections we distinguish between an arbitrary point cloud $P(X, N)$, the input point cloud $P(X^{in}, N^{in})$, output point cloud $P(X^{out}, N^{out})$ and the intermediate point cloud after reconstructing the orientations $P(X^{in}, N^{out})$.

Reweighted ℓ_1. We use in this work a reweighted ℓ_1 scheme in order is to achieve *lower-than-ℓ_1*-sparsity. Such an aggressive sparsity is desired in cases where ℓ_1 is too smooth. Our motivation for using reweighting is drawn from the nature of our problem. For scanned models it is common to have a high correlation of noise in the normals. This effect occurs since normals are commonly approximated using local PCA and it is enhanced since scanners tend to sample more points near sharp edges. While ℓ_1 minimization
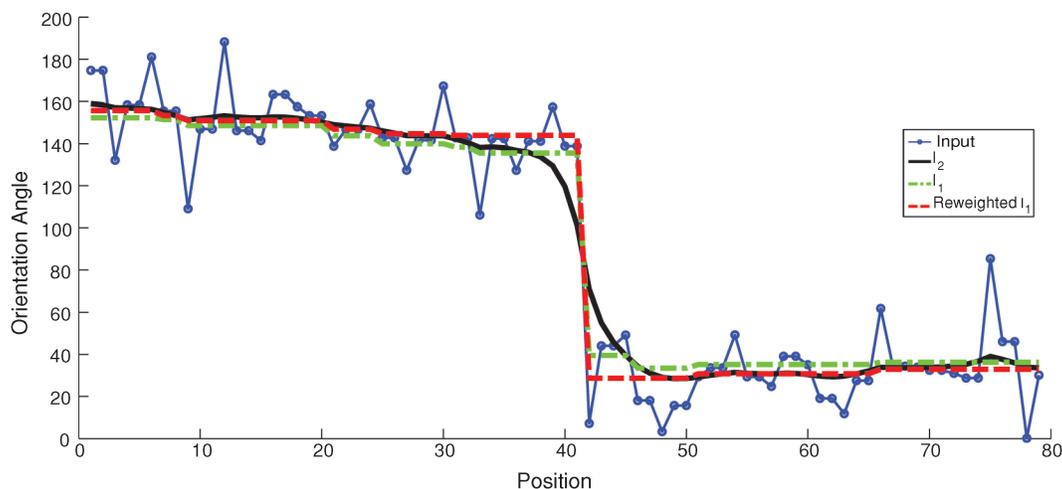
Fig. 3. A comparison of applying ℓ_2 (solid black), ℓ_1 (dotted green) and reweighted-ℓ_1 (dashed red) norms to a set of noisy 2D orientations (circled blue). Sharpness in the reconstruction first appears in the ℓ_1 norm and is enhanced by reweighting.
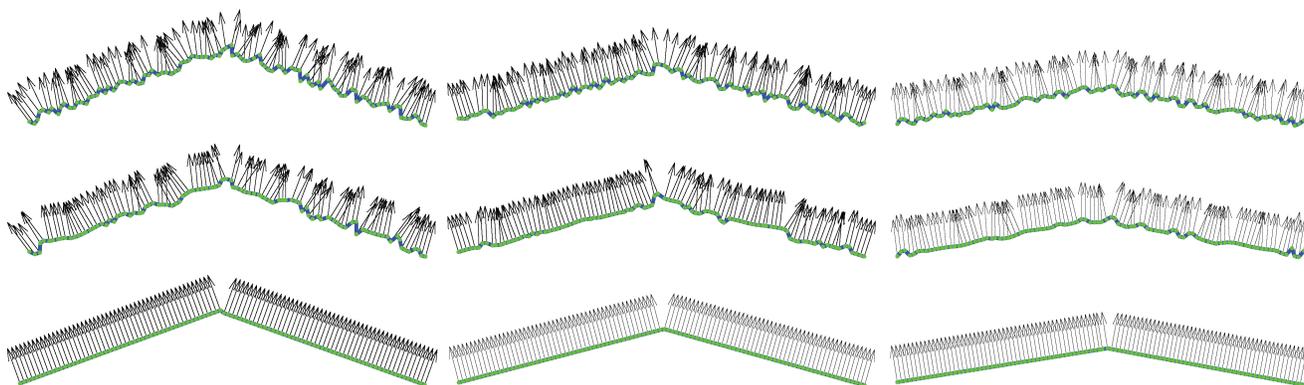

Fig. 4. A comparison between ℓ_1-sparse reconstruction and bilateral filtering applied on a series of synthetic shallow 2D V-shaped models with different signal-to-noise ratios. Top, left-to-right are the noisy inputs with angles $140°$, $150°$, and $160°$ and noise of 1.45%, 1.20%, and 1.00% respectively. Middle is the result of applying a local bilateral filter. Bottom is our ℓ_1-sparse reconstruction.

works well for uncorrelated random noise, it penalizes high values too strongly to break correlation-induced smoothness in the normals.

A higher degree of sparsity can be accomplished by driving the minimization norm below ℓ_1, using a norm ℓ_p, $0 < p < 1$. Unfortunately, such penalty functions are nonconvex. Instead of applying them directly, we use ℓ_1 as the basic building block, and achieve the effect of lower-than-ℓ_1-sparsity using reweighting. Here we rely on the theoretical observations made in Candes et al. [2008], by which reweighting within the ℓ_1 realm may enhance the sparsity and significantly improve the quality of the reconstruction. We can see in Figure 3 that reweighted ℓ_1 is sparser than ℓ_1 and hence achieves a better approximation in this example.

4.1 Orientation Reconstruction

Our orientation minimization consists of two terms: one is the global ℓ_1 minimization of orientation (normal) distances; the second amounts to constraining the solution to be reasonably close to the initial orientations. Following the previous discussion, our minimization term is composed of the normal differences between adjacent points p_i and p_j, formulated as a pairwise penalty function c_{ij}^N.

$$c_{ij}^N(N) = \|n_i - n_j\|_2$$

For a piecewise smooth surface the set $\{c_{ij}^N \geq \tau\}$ is sparse for some small τ depending on the smoothness of the surface, so it makes sense to define a global weighted ℓ_1 penalty function C^N:

$$C^N(N, W, E) = \sum_{(p_i, p_j) \in E} w_{ij} c_{ij}^N(N)$$

where $W = \{w_{ij}\}$ is a set of weights whose role is to achieve lower-than-ℓ_1-sparsity as discussed before, and E is the adjacency set computed using k-nearest neighbors. We perform two ℓ_1 iterations. The first iteration is unweighted. Using the results of the first iteration, we compute weights and resolve. The weights are set to

$$w_{ij} = e^{-(\theta_{ij}/\sigma_\theta)^4},$$

where θ_{ij} is the angle between the initial normals of p_i and p_j and σ_θ is a parameter (usually set to 10 degrees). We use an exponent of 4 instead of the usual 2 for a more aggressive sparsity enhancement.

Notice that $C^N(N, W, E)$ is in fact the ℓ_1 norm of the $|E|$-element vector $[\cdots \; w_{ij}c_{ij}^N(N) \; \cdots]$.

We compute the new orientations as a minimization of the penalty function.

$$N^{out} = \arg\min_N C^N(N, W, E)$$

To avoid the degenerate minimum of $N^{out} = 0$ in our minimization we impose additional constraints on the system. We require change in normal orientation to be within some prescribed expected noise level (γ_n). This comes in the form of imposing a bounded ℓ_∞-norm on the orientation change. We define our global optimization problem by

$$N^{out} = \arg\min_N \sum_{(p_i, p_j) \in E} w_{ij}\|n_i - n_j\|_2$$
$$\text{s.t.} \quad \forall i \, \|n_i - n_i^{in}\|_2 \leq \gamma_n.$$

This is a convex optimization problem. Imposing the additional normalization constraints $\|n_i^{out}\|_2 = 1$ will result in a nonconvex optimization problem. Therefore we solve and renormalize the solution afterwards. Renormalization is usually mild since we constrain orientations in the solution to be close to originals.

Initial orientations. Although our method reconstructs orientations based on their initial values, it does not require them as raw-inputs. Indeed, our implementation loosely approximates orientations from point-positions by applying a local PCA with fixed size neighborhoods. Although more advanced techniques exist for approximating point orientations [Dey and Sun 2006], our algorithm successfully handles coarse initial orientation approximations. Therefore, using such a simple heuristic was sufficient in our case.

4.2 Position Reconstruction

Given the reconstructed normal orientation obtained from the previous step, we reconstruct point position by assuming a local planarity criteria. For each pair of neighbor points $(p_i, p_j) \in E$ we define a penalty function $c_{ij}^X(X, N)$; it measures the projection distance of the points from the local plane defined by their average normal n_{ij} and average position x_{ij}.

$$c_{ij}^X(X, N) = |n_{ij} \cdot (x_i - x_j)|$$

For a piecewise smooth surface the set $\{c_{ij}^X \geq \tau\}$ is sparse for some small τ depending on the smoothness of the surface and sampling resolution, so it makes sense to define a global weighted ℓ_1 penalty function

$$C^X(X, N, W, E) = \sum_{(p_i, p_j) \in E} w_{ij}c_{ij}^X(X, N).$$

The weights $W = \{w_{ij}\}$ are designed to favor smooth parts over nonsmooth parts, so we use the same formula as the one used for orientations, but we recompute them using the new orientation values.

We find the new positions as a minimization of the penalty function where N^{out} is already known and kept fixed.

$$X^{out} = \arg\min_X C^X(X, N^{out}, W, E)$$

To minimize the amount of degrees of freedom we restrict ourselves to movement along normals. This fairly mild restriction has several benefits: it reduces the problem size and avoids the known effect of point clustering. Moreover, in our early experiments, we have noticed no significant benefit in using general movement. Thus, we define reconstructed positions as

$$x_i = x_i^{in} + t_i n_i^{out},$$

and our local penalty functions are

$$c_{ij}^X(X, N^{out}) = |n_{ij}^{out} \cdot (x_i - x_j)| =$$
$$\left|\left(n_{ij}^{out}\right)^T n_i^{out} t_i - \left(n_{ij}^{out}\right)^T n_j^{out} t_j + \left(n_{ij}^{out}\right)^T \cdot \left(x_i^{in} - x_j^{in}\right)\right|. \quad (1)$$

The goal penalty function becomes

$$C^X(X, N^{out}, W, E) = \|At + f\|_1,$$

where $A \in \mathbb{R}^{|E| \times |P|}$ and $f \in \mathbb{R}^{|E|}$ ($|.|$ is the size). Each row of A corresponds to a single $(p_i, p_j) \in E$, and is equal to

$$\left[\cdots \; w_{ij}\left(n_{ij}^{out}\right)^T n_i^{out} \; \cdots \; -w_{ij}\left(n_{ij}^{out}\right)^T n_j^{out} \; \cdots \right].$$

Each index in f corresponds to a single pair $(p_i, p_j) \in E$ and is equal to

$$f_{ij} = \left(n_{ij}^{out}\right)^T \cdot \left(x_i^{in} - x_j^{in}\right).$$

We regularize the problem by constraining the norm of the correction term

$$\|t\|_2 \leq \gamma_x,$$

where γ_x is a parameter proportional to the noise level. We use the following formula to determine γ_x. We have

$$\gamma_x = 0.7 \cdot \eta_x \ell(P)\sqrt{|P|},$$

where $\ell(P)$ is the length of the largest diagonal of the bounding box of the points in P, and η_x is the assumed noise level (in percents of the object size). Our implementation assumes η_x is a parameter provided by the user. Nevertheless, since η_x is directly related to noise, it can be approximated from the local point covariance matrix in the spirit of Pauly et al. [2004].

Overall, to find t we solve the following convex optimization problem.

$$\arg\min_t \|At + f\|_1 \;\; \text{s.t.} \;\; \|t\|_2 \leq \gamma_x$$

5. AN EFFICIENT CONVEX OPTIMIZATION SOLVER

In the previous sections we formulated our method as a sequence of convex optimization problems. These problems are nonlinear, but since they are convex they can be solved efficiently and reliably. Formulating the problem as an ℓ_1 minimization allows us to use an interior-point solver, which usually converges faster than IRLS. We show in Section 6 that our solver is indeed fast and reliable.

The problems described in Section 4 are Second-Order Cone Problems (SOCP). That is, problems of the form

$$\min_x p^T x \;\; \text{s.t.} \;\; \|A_i x + b_i\|_2 \leq c_i^T x + d_i.$$

We now describe a technique for solving the problem described in Section 4.2. A similar technique can be used to solve the problem described in Section 4.1. Nevertheless, for solving orientations we

currently use the external package called CVX [Grant and Boyd 2009], which we found sufficient for our needs.

We recast

$$\arg\min_t \|At + f\|_1 \text{ s.t. } \|t\|_2 \le \gamma_x$$

as the Second-Order Cone Problem (SOCP) by first adding variables $u \in \mathbb{R}^M$. We set $x = (t, u)$ and set $p = (\, 0_{N \times 1} \quad 1_{M \times 1} \,)$. Each row of A adds two inequality constraints

$$A_{i,:}t - u + f_i \le 0$$

and

$$-A_{i,:}t - u + f_i \le 0$$

where $A_{i,:}$ is row i of A. We get the following equivalent SOCP.

$$\min_{t,u} \sum_{i=1}^M u_i \quad \text{s.t.} \quad At - u + f \le 0$$
$$-At - u - f \le 0$$
$$\frac{1}{2}\left(\|t\|_2^2 - \gamma_x^2\right) \le 0$$

where $M = |E|$ (size of adjacency list) and $N = |P|$ (number of points).

We implement a primal solver, using a log-barrier method [Boyd and Vandenberghe 2004; Candes and Romberg 2005]. (See Lobo et al. [1998] for a primal-dual formulation). The method involves solving a series of nonlinear minimization problems of the form

$$(t_k, u_k) = \arg\min_{t,u} \sum_{i=1}^M u_i + \frac{1}{\tau_k} \sum_{i=1}^{2M+1} -\log\left(-g_i\left(t, u\right)\right),$$

where $\tau_k > \tau_{k-1}$ and each g_i corresponds to a constraint in the SOCP (each row of A defines two constraints; the constraint on the size of t is the last constraint). The inequality constraints $\{g_i\}$ have been incorporated into the functional via a penalty function which is infinite when constraints are violated and smooth elsewhere. As τ_k gets large the solution t_k approaches the optimal solution. The method stops when τ_k is large enough, based on the *duality gap* (see Boyd and Vandenberghe [2004] and Candes and Romberg [2005] for more details). Each nonlinear minimization problem is solved iteratively using Newton's method, that is, each Newton iteration involves solving a linear system of equations.

Let us write $g_{(1)} = At - u + f$, $g_{(2)} = -At - u - f$ and $g_{(\gamma)} = \frac{1}{2}(\|t\|_2^2 - \gamma_x^2)$. For a vector v denote by $D(v)$ the diagonal matrix with v on its diagonal, and v^{-1} the vector with the values in v inverted. For our SOCP each Newton iteration involves solving a series of *normal equations* of the form

$$\left(A^T \Sigma_t A - g_{(\gamma)}^{-1} I_{N \times N} + g_{(\gamma)}^{-2} r r^T\right)\Delta t = w_0,$$

where $\Sigma_t = \Sigma_1 - \Sigma_2^2 \Sigma_1^{-1}$, $\Sigma_1 = D(g_{(1)})^{-2} + D(g_{(2)})^{-2}$, $\Sigma_2 = -D(g_{(1)})^{-2} + D(g_{(2)})^{-2}$ and $r = t \in \mathbb{R}^N$ is a dense vector. The solution of the linear system is the *search direction* of the corresponding Newton iteration.

Each Newton step requires the numerical solution of a linear system of equations. It is imperative to solve these equations efficiently, and this requires dealing with sparsity and conditioning issues. The matrix of the normal equations is symmetric positive definite, but for large-scale problems it tends to be ill-conditioned, which in turn may result in an incorrect search direction. Furthermore, the vector r is dense, whereas the original problem is sparse.

Therefore, factoring the matrix using the Cholesky decomposition may require a prohibitive amount of computational work and storage allocation. It is thus preferred, both from a numerical stability point of view and from a sparsity point of view, to adopt an iterative solution technique. We use the LSQR method [Paige and Saunders 1982], which is especially suited for least-squares problems. We write

$$\tilde{A} = \begin{pmatrix} \Sigma_t^{1/2} A \\ (-g_{(\gamma)})^{-1/2} I_{N \times N} \\ g_{(\gamma)}^{-1} r^T \end{pmatrix},$$

and the search direction can now be found by solving

$$\min_{\Delta t} \left\| \tilde{A}\Delta t - w \right\|_2,$$

where

$$w = \begin{pmatrix} \Sigma_t^{-1/2}\left(g_{(1)}^{-1} - g_{(2)}^{-1} - \Sigma_2 \Sigma_1^{-1}\left(\tau_k 1_{N \times 1} + g_{(1)}^{-1} + g_{(2)}^{-1}\right)\right) \\ 0_{N \times 1} \\ 1 \end{pmatrix}.$$

For brevity we omit the formula for w_0, but state that $w_0 = \tilde{A}^T w$.

To deal with the dense row associated with the vector r, we form a preconditioner using the strategy proposed in Avron et al. [2009]. We remove the dense row from $\tilde{A}$; let us call the resulting matrix $\tilde{A}_0$. We then compute the Cholesky factorization of the *sparse* matrix associated with $\tilde{A}_0$:

$$R^T R = \tilde{A}_0^T \tilde{A}_0,$$

using CHOLDMOD [Davis and Hager 2005]. The R factor is used as a preconditioner for the augmented system associated with $\tilde{A}$, and now we apply LSQR. The important point here is that removing r amounts to a rank-1 change of the matrix that corresponds to the least squares operator. Therefore, only two iterations are needed for convergence in exact arithmetic [Avron et al. 2009]. The matrix $\tilde{A}_0^T \tilde{A}_0$ may become very ill-conditioned, which can sometimes cause the Cholesky factorization to fail (by encountering a negative diagonal value due to inaccurate arithmetic). In such cases we use SuiteSparseQR [Davis 2008] to compute a QR factorization instead and use R as a preconditioner.

Finally, we use one additional heuristic to speed up our solver. We have noticed that in some of the iterations, $|g_{(\gamma)}|$ tends to be considerably smaller than the maximum value on the diagonal of Σ_t. In those cases, LSQR on $\tilde{A}$ without a preconditioner tends to converge very quickly, because the singular values of $\tilde{A}$ are strongly clustered. We thus work on $\tilde{A}$ directly when conditioning allows for it (if $\|\Sigma_t\|_2/|g_{(\gamma)}| \ge 10^3$), which saves the cost of a preconditioner solve.

The iterative method stops when the backward error drops below a certain threshold. This ensures backward stability relative to the desired level of accuracy. We use LSQR so the relevant condition number is $\kappa(\tilde{A})$ (and not $\kappa(\tilde{A}^T \tilde{A})$ as is the case for the normal equations). This ensures that a good search directions is found, which is crucial for the log-barrier method, even if low convergence threshold is used. The threshold we used in our experiments is 10^{-8}. As for accuracy of interior-point method, its stopping criteria is based on a threshold as well. Here we found that only a coarse level of accuracy was sufficient and further adjustments had no visual significance.

6. RESULTS AND DISCUSSION

We present results that demonstrate the viability and effectiveness of our method. For rendering purposes, our point set surfaces
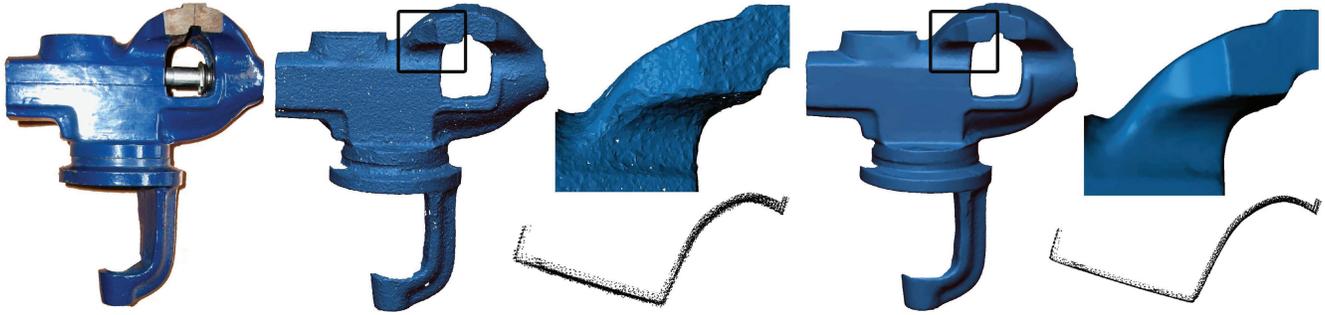
Fig. 5.   Reconstruction of a scanned iron vise. Left to right: the original vise photo; the noisy scan and a zoomed region with its corresponding cross section (bottom); our ℓ_1 reconstructed model; rightmost is the zoomed result, demonstrating the sharp piecewise smooth reconstruction and its cross section (bottom).
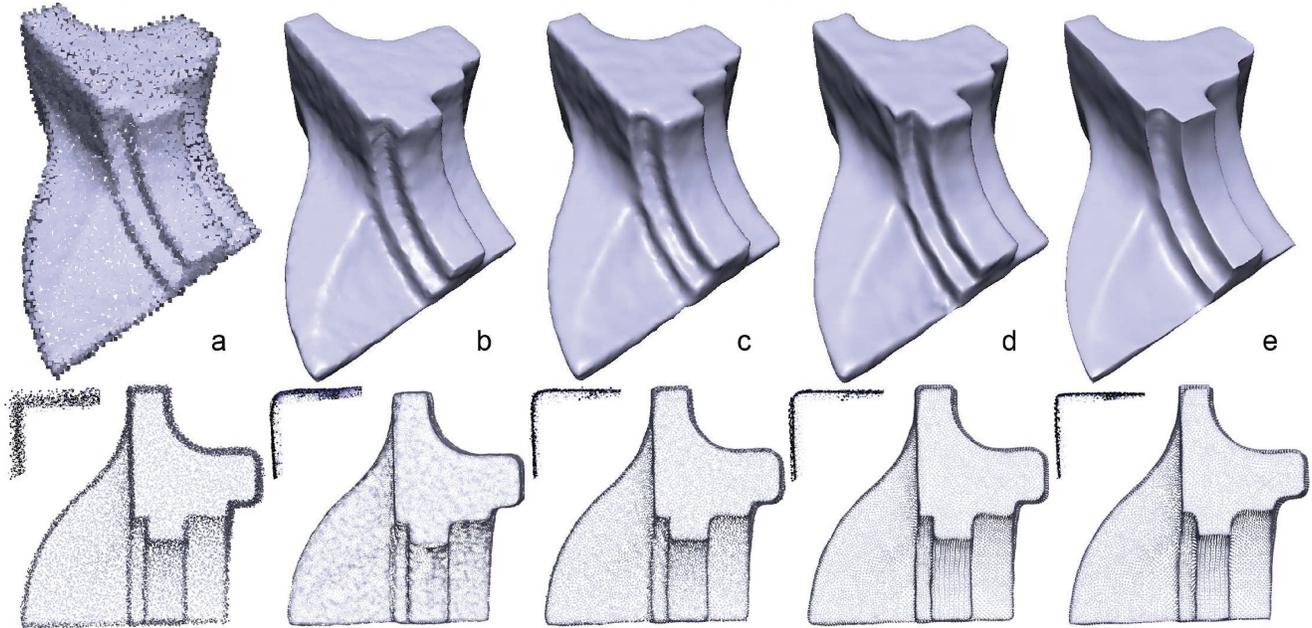

Fig. 6.   Comparison between our ℓ_1 method and state-of-the-art robust reconstruction methods: In (a) we show a noisy fandisk with noise in positions of 1% of the bounding box. Output LOP (b), DDMLS (c), RIMLS (d) and our ℓ_1 method (e). The bottom row contains, for each of the aforesaid, the cross-section of a corner and a top orthographic view.

were meshed using the "Ball Pivoting" algorithm [Bernardini et al. 1999] and rendered using a standard illumination model.

We show in Figure 2 a simple example where we apply our method on a noisy 2D curve to recover its sharp features. In fact, for this simple synthetic model we can accomplish a perfect reconstruction, since it was sampled from a perfect piecewise linear "V" curve. ℓ_1 minimization generates an exact piecewise linear result with one singular point at the apex. For natural, real-world objects, we cannot expect such precise reconstruction. Nevertheless, using our global sparse method we obtain high-quality results even for fairly complex sharp objects with relative high noise level (see Figure 5). The resulting models are piecewise smooth, and the error concentrates on edges, as can be seen in the corresponding zoomed regions and cross sections.

In Figures 6 and 7 we provide a comparison with state-of-the-art feature-aware reconstruction methods applied to the classical fandisk and blade models. In both models, we insert noise in the point positions in the amount of 1% of the bounding box size. In Figure 6, we show the results of LOP [Lipman et al. 2007b], DDMLS [Lipman et al. 2007a], RIMLS [Oztireli et al. 2009], and our method. The superiority of ℓ_1 over the other methods is evident; sharp features are recovered to a high level of accuracy, while smoothness is preserved in other regions.

Figure 7 shows a similar example where local feature-aware reconstruction methods (DDMLS, RIMLS) are able to faithfully recover sharp features (blade edges), however, at the price of erroneously detecting local noise as redundant features (blade facets). Note also the lack of sharpness of some of the corners for the first two methods. In contrast, our global method does not have this flaw, and it correctly locates sparse singularities on the edges in a much cleaner manner.

For all the comparisons, we followed the guidelines provided in the distributed code by the authors and the parameters specified in their publications. We explicitly provide the parameters that we used.
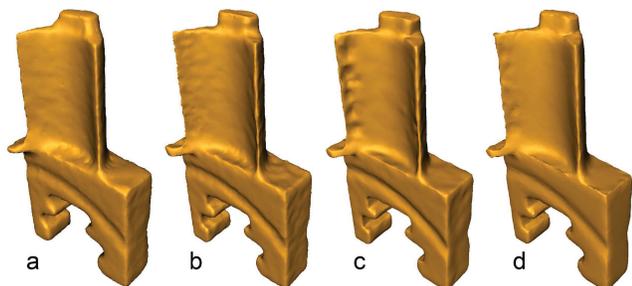
Fig. 7. Comparison between our ℓ_1 with state-of-the-art reconstruction methods applied to a noisy blade model that originally contains sharp edges and smooth parts. We show the reconstruction results of LOP (a), DDMLS (b), RIMLS (c) and our ℓ_1 method (d).
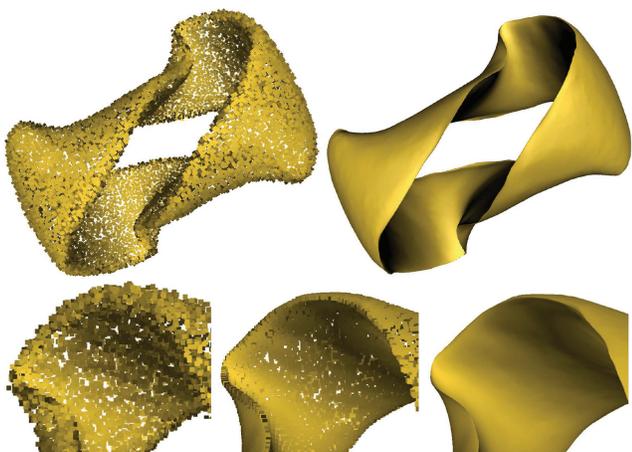

Fig. 8. The ℓ_1 method applied to a sharp knot, with 1% noise added to the positions of the synthetic knot model (top left). The recovered knot appears on the top right. At the bottom, a zoom on a reconstructed sharp edge: from left to right: the initial noisy edge, point cloud after ℓ_1, and reconstruction.

—DDMLS: using cubic piecewise polynomials $m = 3$, local neighborhood size $h = 0.35\%$ of bounding box.

—LOP: max influence radius size $h = 0.3\%$ of bounding box, repulsion parameter $\mu = 0.3$, 10 iterations.

—RIMLS: local weight radii $h = [5 - 7]$ times local point spacing, degree of sharpness $\sigma_n = 0.75$, 15 projection iterations.

Figures 5 and 8 further illustrate the effectiveness of the ℓ_1 approach in terms of recovering the fine features of the object, while leaving the other parts smooth.

We have also applied our method to objects with less evident sharpness in the features. We observe that our method could handle such objects well (Figures 9 and 10). Note that the ability to reconstruct smooth surfaces with no evident sharp features is due to the fact that our norm is ℓ_1 and not purely ℓ_0. In other words, we balance between sparsity and local smoothness. In smooth parts with no evident singularities ℓ_1 minimization acts much like ℓ_2 minimization (much like the way median acts like mean when no outliers are present). In the scanned human face, we compared our global ℓ_1 minimization with a global ℓ_2 minimization. We note that even in this case, where sharpness is low, ℓ_1 provides a result of higher visual quality than ℓ_2.

Fig. 9. Result of applying our method to a scanned funnel (left). The scan contains shallow sharp features that are noisy.

In Figures 9 and 11 we demonstrate the behavior of our method in cases where the signal-to-noise ratio is low in the proximity of sharp features. In Figure 9, we reconstruct a scanned funnel that shows a shallow edge across the model. Figure 11 shows a similar shallow feature along the hand of a scanned Buddha statue. In both examples our method was able to recover sharpness to a large extent without smoothing it.

In Figure 12 we show the result of running the method on a large (240K points) scanned 3D model of a statue based on Escher's famous drawing. It took our solver roughly 20 minutes to compute the optimal global solution. Note that despite its large size, our method does not fall into local minima. Our performance timings are reasonably good, considering the size of the problems. They are in the range of minutes (see Table I) and were measured on a 64-bit Intel Core2 2.1 GHz using MATLAB.

Sensitivity and parameters. Sensitivity to parameters is always a concern for methods of our type. Penalty methods at large require the choice of parameters whose optimal values are often either unknown or prohibitively expensive to compute (e.g., the smallest singular value of a linear operator). This is an area of active research in which progress is constantly being made, but much is still not understood.

Our algorithm is not particularly sensitive to parameters, especially in the positions phase. Table II provides a detailed list of the parameters involved in our method, and the actual range of values used in our experiments. The parameter range is narrow, and use of default parameters along with adjustments of γ_n and η_x according to the perceived noise level yields high-quality results in a consistent fashion. Specifically, to obtain the results in this article we start with the default parameters. Next, based on the amount of noise and sharpness in the results we fine-tuned the parameters to gain further improvement (see Figure 10(c) and 10(d) for a comparison between default and fine-tuned parameters).

We do observe that the parameter that affects the output the most is γ_n. Since γ_n is a measure of noise level, we require a value large enough to obtain correct piecewise smooth normals while avoiding a too high value that may cause oversmoothing. This is a classical signal-to-noise ratio issue, which we explore in Figure 4, which shows three excerpts of a series of shallow V-shaped models of different angles and noise level. As expected, our method can handle less noise as the angle becomes shallower (i.e., weaker signal). The value of γ_n corresponds to noise level: 0.15 for 160°, 0.18 for 150°, and 0.30 for 140°. Like many methods, our method tends to be more sensitive to parameters if the signal-to-noise ratio approaches the method's limit.

Some of this sensitivity may be attributed to the simple approach we use to compute initial orientations, using PCA with constant neighborhoods. In the presence of highly nonuniform sampling
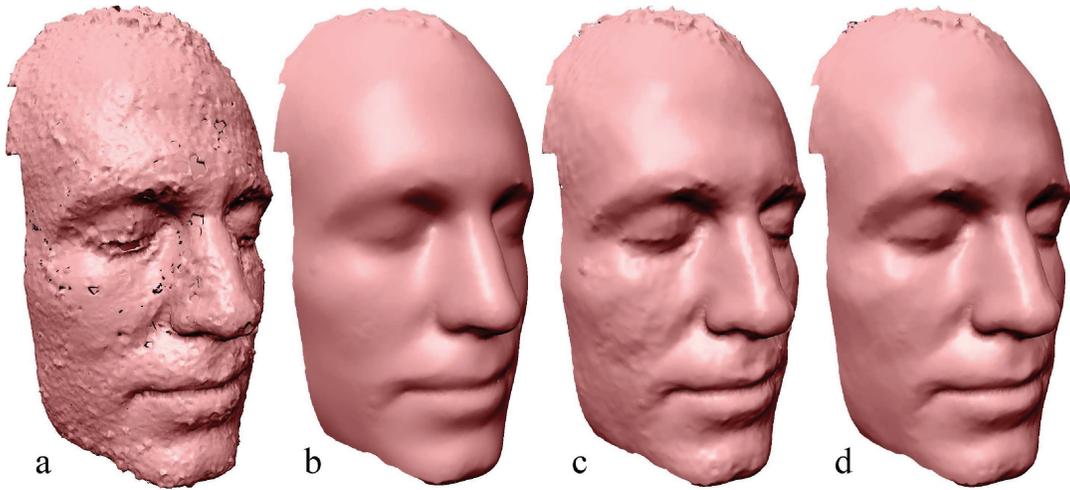
Fig. 10. A comparison of minimization of ℓ_2 norm (b) vs. our ℓ_1-sparse minimization (c, d) on a scanned noisy human face (a). Although there are no pure sharp features, the method works well also on general models. In (c) we show the result of using our default parameters and (d) is obtained after fine-tuning.
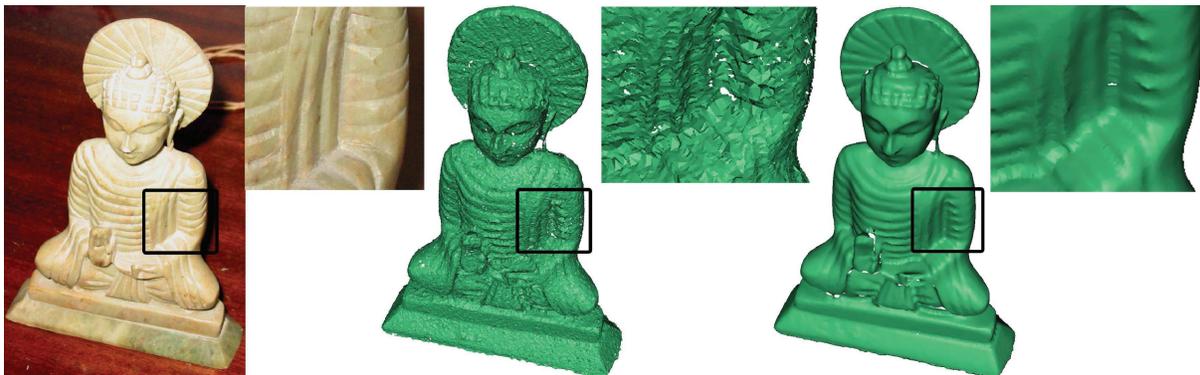

Fig. 11. Result showing our method applied on a noisy scan of the Buddha statue (left). In the zoomed-in regions of the hand, a small sharp feature is present in the original statue. Although hidden by the noise in the scan, our method was capable to pick it using a sparse global representation of the data.
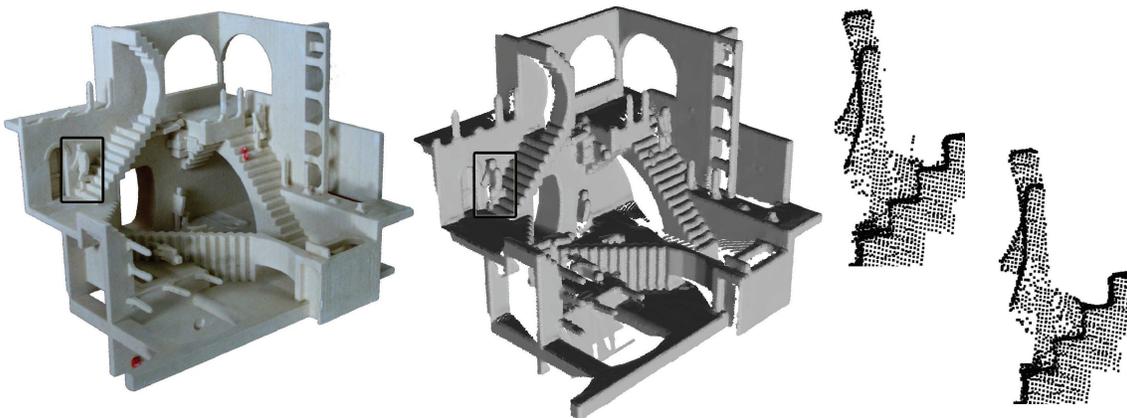

Fig. 12. Result of applying our method to a large 240K noisy point cloud. Left is a highly complex physical model of an Escher statue, middle is the piecewise smooth point cloud after ℓ_1 optimization. On the right we show a zoomed cross-section comparison between the input (top) and our sharp result.

Table I. Running Times

Model	Points	Minutes	Model	Points	Minutes
fandisk	17,106	3.5	*face*	110,551	12
blade	24,998	4	*Buddha*	150,737	27
knot	25,455	7	*funnel*	201,655	21
armadillo	99,416	16	*Escher*	240,909	22

Table II. Parameters

Parameter	Range (Default)
Neighborhood size of normal estimation (k)	$10 - 30$ (20)
Neighborhood size in orientation phase (k)	$3 - 6$ (5)
Max normals correction, 1st iteration (γ_n)	$0.10 - 0.15$ (0.10)
Max normals correction, 2nd iteration (γ_n)	$0.03 - 0.07$ (0.05)
Angle for reweighting, normals phase (σ_θ)	$5° - 20°$ (10°)
Neighborhood size in positions phase (k)	$8 - 12$ (12)
Assumed noise level in positions (η_x)	$0.02 - 0.03$ (0.02)
Angle for reweighting, positions phase (σ_θ)	$4° - 20°$ (10°)

densities and noise, using a more refined technique for initial normals approximation may be more adequate. Finally, global optimization methods tend to be in general more sensitive to parameters than local methods.

On the other hand, our global approach has some clear advantages. Consider again the shallow V-shaped models of Figure 4. With no global considerations, a local method will keep many local sharp features or drop all of them. Using our global ℓ_1 method a single feature that concentrates all the error at one point is a feasible solution even for relatively low signal-to-noise ratios.

Limitations and future work. In some of our synthetic examples, our method has difficulty in correctly projecting points lying exactly on edge singularities. This is because orientations are essentially not defined there. Our method tends to concentrate errors on those edge samples, leaving them as error spikes outside of the model. We observed this phenomenon only in artificially noised synthetic models. This limitation can be overcome in the postprocessing stage, by applying a simple low-pass filter with a very small kernel that removes those singular spikes. For fairness, in our comparisons on synthetic objects we have applied the same filter for any other result that was improved by it. We did not apply the filter to any reconstruction of the real scanned objects.

Another limitation of our method is its relatively high computational cost. Our convex formulation incurs a high cost in the normals computation step, which has been addressed only partially so far. We believe, however, that it is possible to design a very efficient solver. Our experiments show that it is sufficient to solve the nonlinear iterates to a crude tolerance, and hence accelerate convergence, while keeping a high quality of the output. Furthermore, the preconditioner, which is based on a rank-1 correction, preserves sparsity of the underlying operator, and the overall iteration count for the optimization problem is fixed. As part of our future work, we plan to fully optimize our presented convex solver, and we believe that its performance can be improved considerably.

7. CONCLUSIONS

We have introduced an ℓ_1-sparse approach for reconstruction of point set surfaces with sharp features. Our method is based on solving separately for the orientations and the positions and is formulated as a sequence of convex optimization problems. A key point here is that convexity allows for finding a global optimum and deriving efficient solvers. We incorporate a reweighted technique

to further enhance sparsity. A novel iterative solver tailored to the problem and based on a preconditioned iterative solver has been derived and implemented. As we demonstrate on several examples, the results are of high quality.

This work fits within a growing body of literature on methods whose principal goal is to enhance sparsity. We believe that the approach we use and our solution methodology may prove useful and effective for many problems in computer graphics. As part of our future work, we plan to look at extensions and other problems, and optimize the performance of our convex programming solver.

REFERENCES

ADAMSON, A. AND ALEXA, M. 2006. Point-Sampled cell complexes. *ACM Trans. Graph. 25*, 3, 671–680.

ALEXA, M. AND ADAMSON, A. 2004. On normals and projection operators for surfaces defined by point sets. In *Proceedings of the Eurographics Symposium on Point-Based Graphics*. 149–155.

ALEXA, M., BEHR, J., COHEN-OR, D., FLEISHMAN, S., LEVIN, D., AND SILVA, C. T. 2003. Computing and rendering point set surfaces. *IEEE Trans. Visualiz. Comput. Graph. 9*, 1, 3–15.

AMENTA, N. 2004. Defining point-set surfaces. *ACM Trans. Graph.* 264–270.

AMENTA, N. AND KIL, Y. J. 2004. The domain of a point set surfaces. In *Proceedings of the Eurographics Symposium on Point-based Graphics 1*, 1, 139–147.

AVRON, H., NG, E., AND TOLEDO, S. 2009. Using perturbed QR factorizations to solve linear least-squares problems. *SIAM J. Matrix Anal. Appl. 31*, 2, 674–693.

BERNARDINI, F., MITTLEMAN, J., RUSHMEIER, H., SILVA, C., AND TAUBIN, G. 1999. The ball-pivoting algorithm for surface reconstruction. *IEEE Trans. Visualiz. Comput. Graph. 5*, 4, 349–359.

BOYD, S. AND VANDENBERGHE, L. 2004. *Convex Optimization*. Cambridge University Press.

CANDES, E. AND ROMBERG, J. 2005. l1-Magic : Recovery of sparse signals via convex programming. In http://www.acm.caltech.edu/l1magic/.

CANDES, E. J., ROMBERG, J., AND TAO, T. 2006. Robust uncertainty principles: exact signal reconstruction from highly incomplete frequency information. *IEEE Trans. Inf. Theory 52*, 2, 489–509.

CANDES, E. J. AND WAKIN, M. B. 2008. An introduction to compressive sampling [a sensing/sampling paradigm that goes against the common knowledge in data acquisition]. *IEEE Signal Process. Mag. 25*, 2, 21–30.

CANDES, E. J., WAKIN, M. B., AND BOYD, S. P. 2008. Enhancing sparsity by reweighted l1 minimization. *J. Fourier Anal. Appl. 14*, 877–905.

CHAN, T. F., OSHER, S., AND SHEN, J. 2001. The digital TV filter and nonlinear denoising. *IEEE Trans. Image Process. 10*, 231–241.

CHEN, S. S., DONOHO, D. L., AND SAUNDERS, M. A. 2001. Atomic decomposition by basis pursuit. *SIAM Rev. 43*, 1, 129–159.

CLAERBOUT, J. AND MUIR, F. 1973. Robust modeling of erratic data. *Geophys. 38*, 5, 826–844.

DANIELS, J. I., HA, L. K., OCHOTTA, T., AND SILVA, C. T. 2007. Robust smooth feature extraction from point clouds. In *Proceedings of the IEEE International Conference on Shape Modeling and Applications (SMI'07)*. 123–136.

DAVIS, T. A. 2008. Multifrontal multithreaded rank-revealing sparse qr factorization. *ACM Trans. Math. Softw.*

DAVIS, T. A. AND HAGER, W. W. 2005. Row modifications of a sparse cholesky factorization. *SIAM J. Matrix Anal. Appl. 26*, 3, 621–639.

DEY, T. K. AND SUN, J. 2005. An adaptive mls surface for reconstruction with guarantees. In *Proceedings of the 3rd Eurographics Symposium on Geometry Processing (SGP'05)*. 43.

DEY, T. K. AND SUN, J. 2006. Normal and feature approximations from noisy point clouds. Lecture Notes in Computer Science, vol. 4337. Springer, 21–32.

DONOHO, D. L., ELAD, M., TEMLYAKOV, V. N., AND A. 2006. Stable recovery of sparse overcomplete representations in the presence of noise. *IEEE Trans. Inf. Theory 52*, 6–18.

ELAD, M., STARCK, J., QUERRE, P., AND DONOHO, D. 2005. Simultaneous cartoon and texture image inpainting using morphological component analysis (mca). *Appl. Comput. Harmonic Anal. 19*, 3, 340–358.

ELSEY, M. AND ESEDOGLU, S. 2009. Analogue of the total variation denoising model in the context of geometry processing. *Multiscale Model. Simul. 7*, 4, 1549–1573.

FLEISHMAN, S., COHEN-OR, D., AND SILVA, C. T. 2005. Robust moving least-squares fitting with sharp features. *ACM Trans. Graph. 24*, 3, 544–552.

FLEISHMAN, S., DRORI, I., AND COHEN-OR, D. 2003. Bilateral mesh denoising. *ACM Trans. Graph. 22*, 3, 950–953.

GRANT, M. AND BOYD, S. 2009. CVX: Matlab software for disciplined convex programming. http://stanford.edu/boyd/cvx.

GUENNEBAUD, G. AND GROSS, M. 2007. Algebraic point set surfaces. In *Proceedings of the ACM SIGGRAPH'07 Conferenec*.

HOLLAND, P. AND WELSCH, R. 1977. Robust regression using iteratively reweighted least-squares. *Commu. Statist. Theory Methods 6*, 9, 813–827.

JONES, T. R., DURAND, F., AND DESBRUN, M. 2003. Non-Iterative, feature-preserving mesh smoothing. In *ACM SIGGRAPH Papers*. 943–949.

KOLLURI, R. 2005. Provably good moving least squares. In *Proceedings of the 16th Annual ACM-SIAM Symposium on Discrete Algorithms (SODA'05)*. 1008–1017.

LEVIN, A., FERGUS, R., DURAND, F., AND FREEMAN, W. T. 2007. Image and depth from a conventional camera with a coded aperture. In *SIGGRAPH Papers*. ACM.

LEVIN, D. 2003. Mesh-independent surface interpolation. In *Geometric Modeling for Scientific Visualization*. 37–49.

LIPMAN, Y., COHEN-OR, D., AND LEVIN, D. 2007a. Data-dependent mls for faithful surface approximation. In *Proceedings of the 5th Eurographics Symposium on Geometry Processing (SGP'07)*. 59–67.

LIPMAN, Y., COHEN-OR, D., LEVIN, D., AND TAL-EZER, H. 2007b. Parameterization-free projection for geometry reconstruction. *ACM Trans. Graph. 26*, 3, 22.

LIPMAN, Y., SORKINE, O., LEVIN, D., AND COHEN-OR, D. 2005. Linear rotation-invariant coordinates for meshes. In *Proceedings of ACM SIGGRAPH*. 479–487.

LOBO, M. S., VANDENBERGHEB, L., BOYD, S., AND LEBRET, H. 1998. Applications of second-order cone programming. *Linear Algeb. Appl. 284*, 193–228.

MEDEROS, B., VELHO, L., AND DE FIGUEIREDO, L. H. 2003. Robust smoothing of noisy point clouds. In *Proceedings of the SIAM Conference on Geometric Design and Computing*.

OZTIRELI, C., GUENNEBAUD, G., AND GROSS, M. 2009. Feature preserving point set surfaces based on non-linear kernel regression. *Comput. Graph. Forum 28*, 2, 493–501.

PAIGE, C. C. AND SAUNDERS, M. A. 1982. LSQR: An algorithm for sparse linear equations and sparse least squares. *ACM Trans. Math. Softw. 8*, 1, 43–71.

PAULY, M., KEISER, R., AND GROSS, M. H. 2003. Multi-Scale feature extraction on point-sampled surfaces. *Comput. Graph. Forum 22*, 3, 281–290.

PAULY, M., MITRA, N., AND GUIBAS, L. 2004. Uncertainty and variability in point cloud surface data. In *Symposium on Geometry Processing (SGP'04)*.

REUTER, P., JOYOT, P., TRUNZLER, J., BOUBEKEUR, T., AND SCHLICK, C. 2005. Point set surfaces with sharp features. Tech. rep., LaBRI.

RUDIN, L., OSHER, S., AND FATEMI, E. 1992. Nonlinear total variation based noise removal algorithms. *Physica D 60*, 259–268.

RUDIN, L. I. 1987. Images, numerical analysis of singularities and shock filters. Tech. rep. California Insitute of Technology.

SHARF, A., ALCANTARA, D. A., LEWINER, T., GREIF, C., SHEFFER, A., AMENTA, N., AND COHEN-OR, D. 2008. Space-time surface reconstruction using incompressible flow. In *ACM SIGGRAPH Papers*. vol. *27*, 1–10.

SHEN, C., OBRIEN, J. F., AND SHEWCHUK, J. R. 2004. Interpolating and approximating implicit surfaces from polygon soup. In *ACM Trans. Graph*. 896–904.

SHEPARD, D. 1968. A two-dimensional interpolation function for irregularly-spaced data. In *Proceedings of the 23rd ACM National Conference*. 517–524.

STARCK, J.-L., ELAD, M., AND DONOHO, D. L. 2005. Image decomposition via the combination of sparse representations and a variational approach. *IEEE Trans. Image Process. 14*, 10, 1570–1582.

TASDIZEN, T., WHITAKER, R., BURCHARD, P., AND OSHER, S. 2002. Geometric surface smoothing via anisotropic diffusion of normals. In *Proceedings of the Conference on Visualization (VIS'02)*. IEEE Computer Society, 125–132.

TASDIZEN, T., WHITAKER, R., BURCHARD, P., AND OSHER, S. 2003. Geometric surface processing via normal maps. *ACM Trans. Graph. 22*, 4, 1012–1033.

TOMASI, C. AND MANDUCHI, R. 1998. Bilateral filtering for gray and color images. In *Proceedings of the 6th International Conference on Computer Vision (ICCV'98)*. 839.

TROPP, J. A. 2006. Just relax: Convex programming methods for identifying sparse signals in noise. *IEEE Trans. Inf. Theory 52*, 3, 1030–1051.